Solid-State Structure and Properties of Hyperbranched Polyols

M. ROGUNOVA,[1] T.-Y. S. LYNCH,[2] W. PRETZER,[2] M. KULZICK,[2] A. HILTNER,[1] E. BAER[1]

[1] Department of Macromolecular Science and Center for Applied Polymer Research, Case Western Reserve University, Cleveland, Ohio 44106-7202

[2] Amoco Chemicals, Naperville, Illinois 60566-7011

Received 14 October 1999; accepted 16 November 1999

ABSTRACT: Structure–property relationships were studied in a series of hyperbranched polyesters based on dimethoxypropionic acid with ethoxylated pentaerythritol as the core. In DSC thermograms, all the polyols exhibit a prominent glass transition and a small melting endotherm. It is possible to model the glass transition temperature of hyperbranched polymers by adapting a method used to calculate the glass transition temperature of dendritic polymers. Because the glass transition occurs near ambient temperature, small changes in the glass transition temperature with generation number have a large effect on the mechanical properties. Polyols that are above the glass transition temperature are ductile. Polyols that are below the glass transition temperature are brittle. When deposited from a dilute solution, the polyols form monolayer aggregates of spherical molecules. The aggregates are stabilized by hydrogen bonding of terminal repeat units. The observation of a yield stress indicates that the intermolecular associations provide a level of resistance to deformation. However, because the globular structure does not permit the usual processes of orientation and strain hardening, the neck gradually thins until it fractures at an engineering strain above 100%.
 J Appl Polym Sci 77: 1207–1217, 2000

Key words: hyperbranched polyols; starburst polymers; polyesters; structure–property relationships

INTRODUCTION

Since the development of the synthetic pathways in the refs. 1–3, dendrimers and hyperbranched polymers have attracted considerable attention. These highly branched macromolecules are characterized by a globular structure with a multiplicity of reactive end groups.[4–6] Consequently, dendrimers and hyperbranched polymers differ significantly from conventional linear polymers in their physical properties. Because hyperbranched polymers are synthesized through a one-step polycondensation reaction, their branching is irregular and they exhibit broad molecular weight distributions. Structurally, hyperbranched polymers can be thought of as intermediate between linear polymers and symmetrically perfect dendrimers.

Hyperbranched polymers are attractive because they resemble dendritic polymers, but they can be produced more easily on a larger scale at a reasonable cost.[7,8] Previous research focused on development of synthetic approaches for specific systems, and subsequent characterization emphasized the thermal and rheological behavior.[9,10] A number of unusual features have been reported, such as significantly lower viscosity compared to

Correspondence to: A. Hiltner.
Contract grant sponsor: Amoco Chemical Co.

Journal of Applied Polymer Science, Vol. 77, 1207–1217 (2000)

linear polymers of the same molecular weight.[11] Another characteristic of hyperbranched polymers is their very high solubility in a variety of solvents.[12] Less is known about the solid-state properties including the mechanical behavior of hyperbranched polymers.

The unique architecture of dendritic and hyperbranched polymers opens avenues to new concepts in structure–property relationships. Because of their ready availability, a series of hyperbranched polyesters based on dimethoxypropionic acid with hydroxyl end groups was studied. The present work focused on the solid-state structure and its relationship to thermal and mechanical properties. Using generation number as a variable, correlations were sought between structure (molecular mass, molecular size, and shape) and properties (thermal behavior, mechanical properties) in order to identify potential areas of application.

EXPERIMENTAL

Materials

Four hyperbranched polyesters based on dimethoxypropionic acid (bis-MPA) as the repeating unit and ethoxylated pentaerythritol as the tetrafunctional core were obtained from Perstorp Polyols (Perstop, Sweden).[13] The pseudo-one-step procedure involves sequential addition of a monomer, each addition corresponding to the stoichiometric amount of the next theoretical generation. The polymers are identified by generation as second, third, fourth, and fifth in accordance with the stoichiometric ratio between core and repeating units. Because the growth of a hyperbranched molecule occurs randomly, the hyperbranched polymers are not ideal in the sense that some monomer units are linearly incorporated. The repeating unit, bis-MPA, is incorporated into polyols in three ways: as dendritic units that are fully esterified with no unreacted hydroxyls, as linear units with one unreacted hydroxyl group, and as terminal units with two unreacted hydroxyls (Fig. 1). The ratio of the number of dendritic and terminal units to the total number of units defines the degree of branching (DB):

$$\mathrm{DB} = \frac{\sum \text{dendritic} + \sum \text{terminal}}{\sum \text{dendritic} + \sum \text{terminal} + \sum \text{linear}} \quad (1)$$

The molecular weight, hydroxyl functionality (number of unreacted hydroxyl groups), and DB are listed in Table I.

Methods

The thermal stability and volatile content were determined on the as-received granules. Specimens weighting 10–15 mg were heated in a Perkin–Elmer Model 7 TGA to 600°C at a rate of 10°C/min. The purge gas was a mixture of N_2 (55%) and O_2 (45%). Loss of volatiles was observed as a weight loss between 100 and 200°C. The amount of volatiles was determined from the weight loss measured at the intersection of two tangential lines.

As-received granules were dried in a vacuum for 8 h at 40°C and compression-molded into films 0.8 mm thick. The dry granules were sandwiched between Teflon sheets and heated at 120°C for 5 min under minimal pressure and for 5 min at 375 psi. The films were cooled under pressure at a rate of 15°C/min. These films were used for density, differential scanning calorimetry (DSC), wide-angle X-ray diffraction, and mechanical measurements.

The density of small pieces cut from the films was measured with a hydrometer using chloroform/hexane solutions. At least three specimens were tested for each material. There was a small increase in the density with the generation number from 1.285 g/cc for polyol-2 to 1.305 g/cc for polyol-5 (Table II).

Samples weighting 4–10 mg were cut from the films for thermal analysis in a Perkin–Elmer Model 7 DSC. The specimens were heated from 25 to 40°C at 10°C/min and held at 40°C for 10 min to remove the thermal history. They were subsequently slowly cooled to −50°C at a rate of 1°C/min and held 3 min at −50°C. The thermogram was recorded as the specimen was heated from −50 to 100°C at 10°C/min (first heating), cooled to −50°C at 10°C/min, and reheated to 100°C at 10°C/min (second heating).

Wide-angle X-ray diffraction patterns were recorded with a Statton camera using CuKα radiation from a Philips PW 1830 generator. The intensity was recorded with a Philips 3100 diffractometer.

Stress–strain behavior was measured in uniaxial tension with ASTM 1708 microtensile specimens cut from the compression-molded films. The gauge length was 22.25 mm; the specimen width was 4.8 mm. Specimens were stretched in an Instron 1123 with strain rates of 1, 10, 100, and 1000%/min.

The polyols were deposited on mica substrates for atomic force microscopy (AFM). The freshly

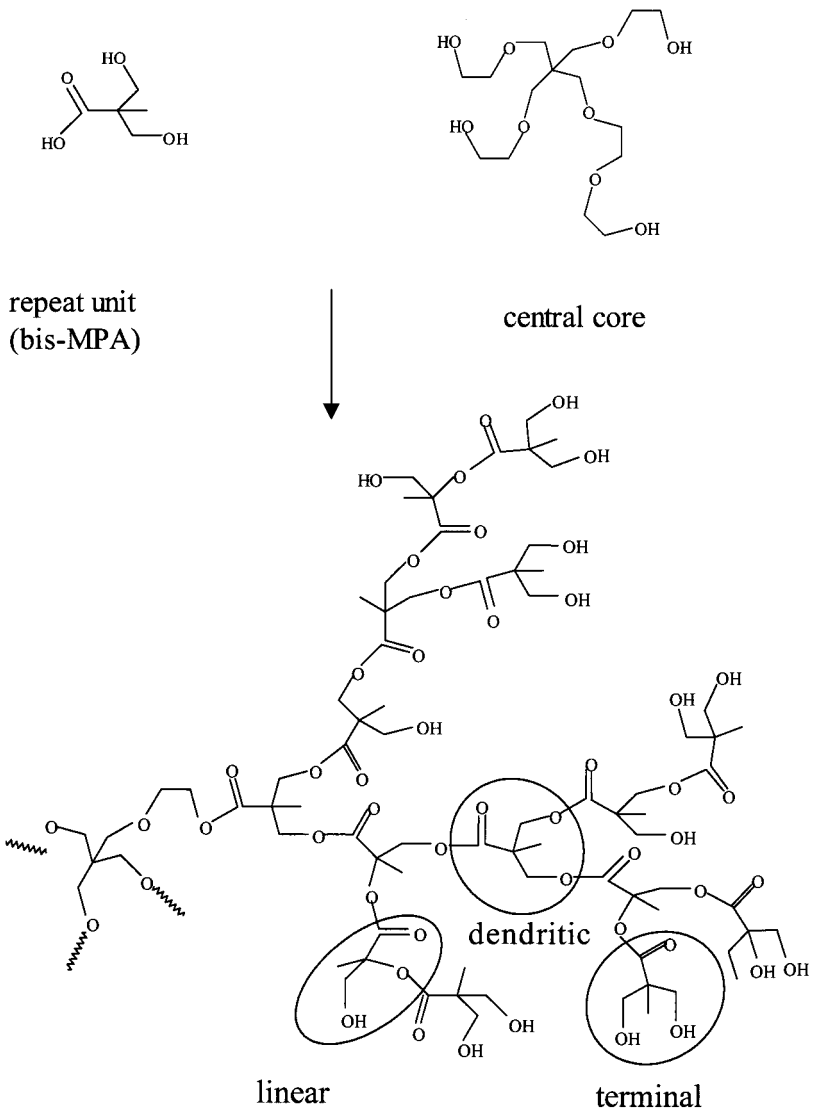

Figure 1 Schematic representation of the hyperbranched polyol molecule.

cleaved mica substrate was immersed in a dilute solution of the polyol in THF (3 μg/mL) for 2 min and dried at ambient temperature in a vacuum for 30 min. The AFM experiments were conducted in air with a commercial scanning probe microscope Nanoscope IIIa from Digital Instruments (Santa Barbara, CA) operating in the tapping mode. Measurements were performed at ambient

Table I Characteristics of Hyperbranched Polyols[a]

Designation	Type	M_w Calculated	M_w by SEC	Hydroxyl-Functionality	Degree of Branching (%)
Polyol-2	2nd generation	1750	1800	16	45
Polyol-3	3rd generation	3600	3300	32	45
Polyol-4	4th generation	7300	5900	64	44
Polyol-5	5th generation	14,800	6700	128	44

[a] Data from Perstorp Polyols.

Table II Physical Properties of Hyperbranched Polyols

Designation	Volatiles (%)	Density (g/cm^3)	T_g (K)	T_m (K)	ΔH (J/g)
Polyol-2	2.5	1.285	274	328	4.3
Polyol-3	1.5	1.295	283	330	9.1
Polyol-4	1.5	1.300	295	331	5.9
Polyol-5	1.4	1.305	300	331	7.0

conditions using rectangular diving-board-type Si probes with a spring constant of 50 N/m and resonance frequencies in the 284–362 kHz range. The tip radius was 10 nm.

RESULTS AND DISCUSSION

Characterization

The polyols exhibited good thermal stability. A small decrease in weight beginning at about 100°C was attributed to the loss of volatiles; the onset of degradation followed at ~ 250°C. The thermal stability improved only slightly as the polyol generation increased from 2 to 5 (Table II). The amount of volatiles was about 2.5 wt % for polyol-2 and 1.5 wt % for the other polyols.

First heating thermograms of all the polyols showed a glass transition and a melting endotherm (Fig. 2). The temperature of the prominent glass transition increased with generation from below ambient temperature for polyol-2 (1°C) and polyol-3 (10°C) to about or above ambient temperature for polyol-4 (22°C) and polyol-5 (27°C). The glass transition temperature for dendritic systems has been reported to increase with generation number to a limit, above which it remains practically constant.[14] In the hyperbranched system, the increase in T_g with generation number is assumed to reflect a decrease in chain mobility due to branching. Therefore, the glass transition temperature depends on the microstructure of the arm emerging from the central core.

Because of the large number of chain ends, the chemical nature of the terminal groups strongly affects the glass transition temperature. For example, the glass transition of a similar polyol decreases from 32 to 15°C if converted to the benzoate and decreases to −20°C as the propionate.[15] The glass transition temperature also depends on the microstructure of the arm emerging from the central core as determined by the composition of the polymer backbone, the number of unreacted end groups, and the degree of branching. In contrast to the linear polymer, where chain ends affect the glass transition temperature only at low molecular weight, the hyperbranched macromolecule has an ever-increasing number of chain ends, which decreases the glass transition temperature, and, concurrently, an ever-increasing number of branching points, which

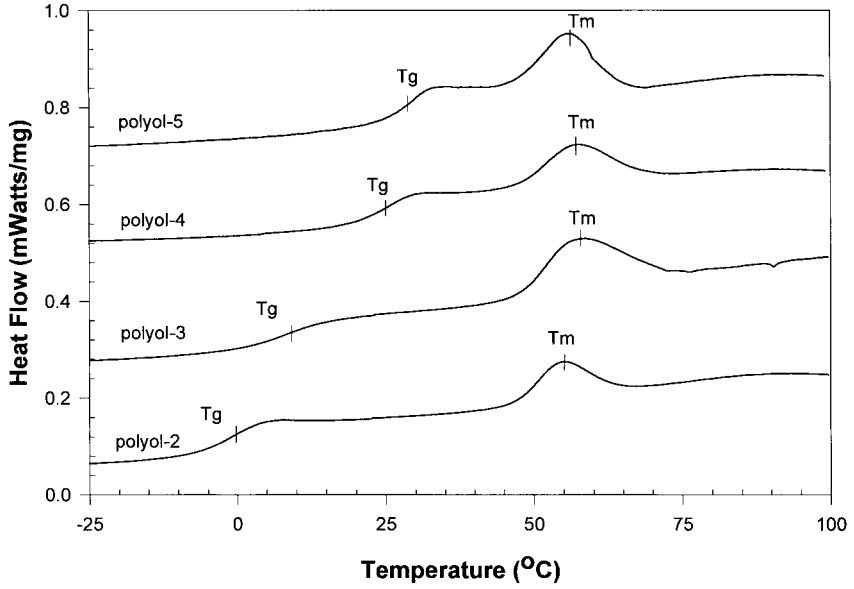

Figure 2 DSC thermograms of polyols.

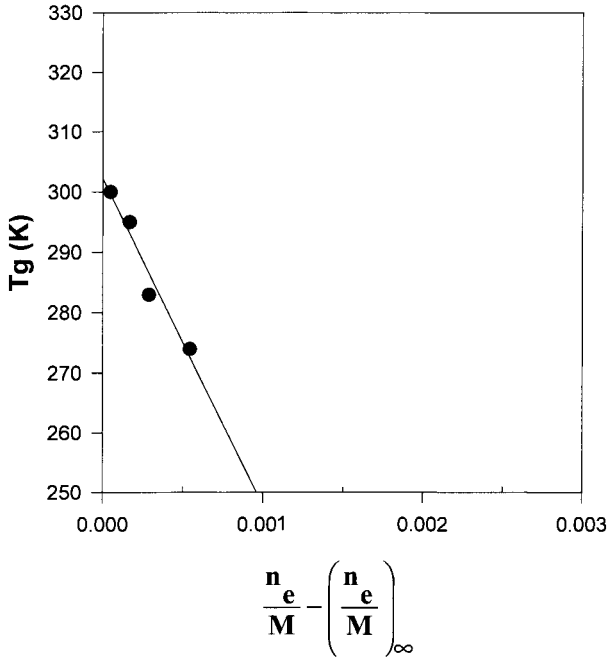

Figure 3 Glass transition temperature of polyols versus $[n_e/M - (n_e/M)_\infty]$.

restricts segmental mobility and increases the glass transition temperature.

One approach to modeling the glass transition of dendritic polymers derives from the chain effect for linear polymers[14]:

$$T_g = T_g^\infty - K\left(\frac{n_e}{M}\right) \quad (2)$$

where T_g^∞ is the value of T_g extrapolated to infinite molecular weight; K, a constant that depends on chain-end free volume and density; n_e, the number of chain ends per molecule; and M, the molecular weight. Because dendritic and hyperbranched macromolecules have an ever-increasing number of chain ends, n_e and M both increase with the generation number. Therefore, the ratio n_e/M does not approach zero at high molecular weight, and unlike linear polymers, T_g^∞ cannot be obtained by extrapolation to $n_e/M = 0$. However, the ratio n_e/M reaches a limiting value $(n_e/M)_\infty$ at high molecular weight. Subtracting this additional term, eq. (2) becomes

$$T_g = T_g^\infty - K\left[\frac{n_e}{M} - \left(\frac{n_e}{M}\right)_\infty\right] \quad (3)$$

Table III Parameters of T_g Calculation

Designation	T_g^∞ (K)	F_{tot}	F_{react}	p
Polyol-2	256	9	9 − 4 = 5	0.556
Polyol-3	259	21	21 − 8 = 13	0.619
Polyol-4	260	45	45 − 16 = 29	0.644
Polyol-5	262	93	93 − 32 = 61	0.656

The value of $(n_e/M)_\infty$ depends on the molecular weight of the monomer unit and the branch multiplicity. For the polyols, (n_e/M) decreased slightly with M, leveling off at a value of 0.0086. Using this as $(n_e/M)_\infty$, the data fit eq. (3) with a correlation coefficient of 0.96 and extrapolation gave $T_g^\infty = 29°C$ and $K = 5.6 \times 10^4$ K g/mol (Fig. 3). These values are close to those reported for dendritic poly(benzyl ethers).[10]

An alternative expression for the glass transition that incorporates the additional influence of branch density is[16]

$$T_g = [T_g^\infty - K_1(1-p)]\left(1 + K_2\frac{X_c}{1-X_c}\right) \quad (4)$$

where T_g^∞ is the glass transition temperature of the linear polymer of infinite molecular weight; K_1, a constant characterizing the influence of end

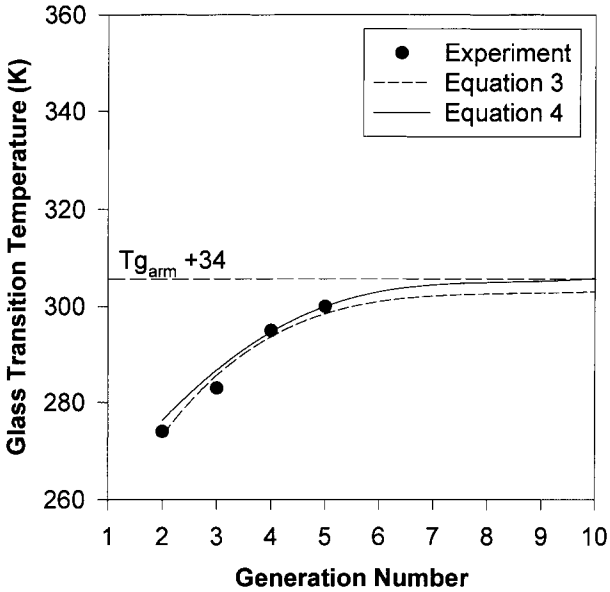

Figure 4 Glass transition temperature of polyols compared with predictions from (solid line) eq. (4) and (dashed line) eq. (3).

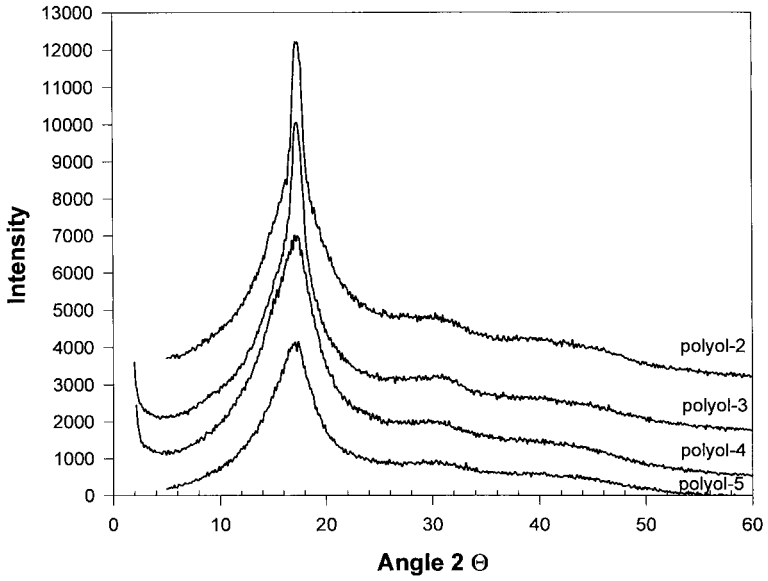

Figure 5 X-ray diffractometer scans of polyols.

groups; K_2, a constant characterizing the influence of branches; X_c, the branch density; and p, the fractional conversion defined as the ratio of reacted functional groups to the total number of functional groups. The reference glass transition T_g^∞ of the hyperbranched polyol changes with the generation number because the initiator core and branching unit are different (copolymer effect). The value of T_g^∞ for each generation was calculated using the Fox equation:

$$\frac{1}{T_{g_i}^\infty} = \frac{w_c}{T_{g_c}} + \frac{w_r}{T_{g_r}} \tag{5}$$

where w_c and w_r are the weight fractions of the core and arms, respectively. The structural analog for the core is poly(vinyl methyl ether), $[—(CH_2)—O—(CH_2)_2]_n$, with $T_{g_c} = 242$ K.[17] For the arms, the analog is $[—CH_2—C(CH_3)_2—COO—]_n$, with $T_{g_r} = 263$ K.[18] The values of T_g^∞ calculated from eq. (5) are included in Table III.

At complete reaction, the fractional conversion of the bis-MPA monomer p is given by[16]

$$p = \frac{F_{\text{react}}}{F_{\text{tot}}} = \frac{2^{(g-1)} + 3\sum_{g=1}^{g-1} 2^{(g-1)}}{3\sum_{g=1}^{g} 2^{(g-1)}} \tag{6}$$

where g is the generation number (Table III).

The branch density X_c is defined as the fraction of bis-MPA units present as branch points and is the ratio of the number of branched units to the sum of the terminal, branched, and linear units. The branch density was obtained from the degree of branching (Table I). Including the central core with two branch units, the branch density was the same for each generation and equal to 0.25.

The constant K_1 reflects the molecular weight dependence. For linear aliphatic polyesters, K_1 is not very sensitive to structure and a typical value of $K_1 = 98$ was used.[19] The branching constant K_2, which characterizes the influence of branch density on the glass transition temperature, was used as a fitting parameter. The value of K_2 is similar for many crosslinked polymers and equal to about 1.2.[19] Using a slightly lower value of $K_2 = 1.0$, eq. (4) satisfactorily described the increase in T_g with the generation number (Fig. 4).

Both approaches predicted leveling off of T_g at higher generations. The beginning of leveling off is apparent in the T_g of polyol-5. The dependency of T_g on the generation number and the limiting value of T_g^∞ obtained by the two methods were almost the same (Fig. 4). The value of T_g^∞ was 30°C from eq. (3) compared to 34°C from eq. (4). A similar leveling-off trend in linear polymers is associated with the decreasing number of chain ends as the molecular weight increases.[19] Leveling off in hyperbranched polymers results from

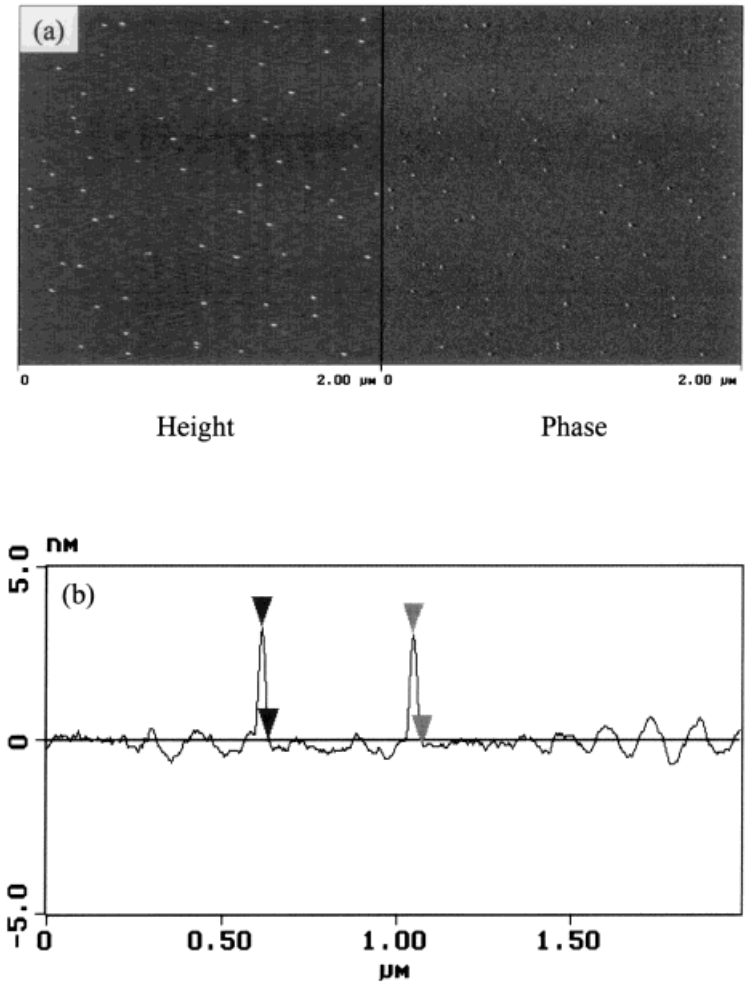

Figure 6 AFM images and section analysis of polyol-5 on mica.

two factors that contribute in opposite ways to the glass transition temperature. Unreacted functional groups decrease the glass transition temperature below that of the linear analog. This is analogous to the molecular weight effect in linear polymers. On the other hand, branching increases the glass transition temperature. The effects of end groups and branches compensate each other to some extent. It can be seen from eq. (4) that the fractional conversion p initially increases with the generation number but rapidly approaches a limiting value of $p = 0.667$ after the fifth or sixth generation. Therefore, if the constancy in branch density ($X_c = 0.25$) extends to higher generation numbers, the glass transition temperature should level off. Branching more than compensates for chain ends, and the glass transition temperature levels off at a value about 44° above the glass transition of the linear analog.

Solid-State Structure

The wide-angle X-ray pattern consisted of a strong crystalline reflection with a spacing of 0.473 nm and a weak amorphous reflection with a spacing of about 0.26 nm. As seen from the defractometer scans in Figure 5, the generation number did not affect the spacing of the crystalline band; however, the intensity and sharpness decreased with an increasing generation number, which suggested a loss of crystalline order with an increasing generation number.

A similar reflection with a spacing of 0.47 nm in the diffraction pattern of linear aliphatic polyesters is assigned to the intermolecular spacing of chains in the planar zigzag configuration.[20] Because the hyperbranched molecule grows randomly, linear crystallizable monomer runs are possible. The degree of branching, about 0.45

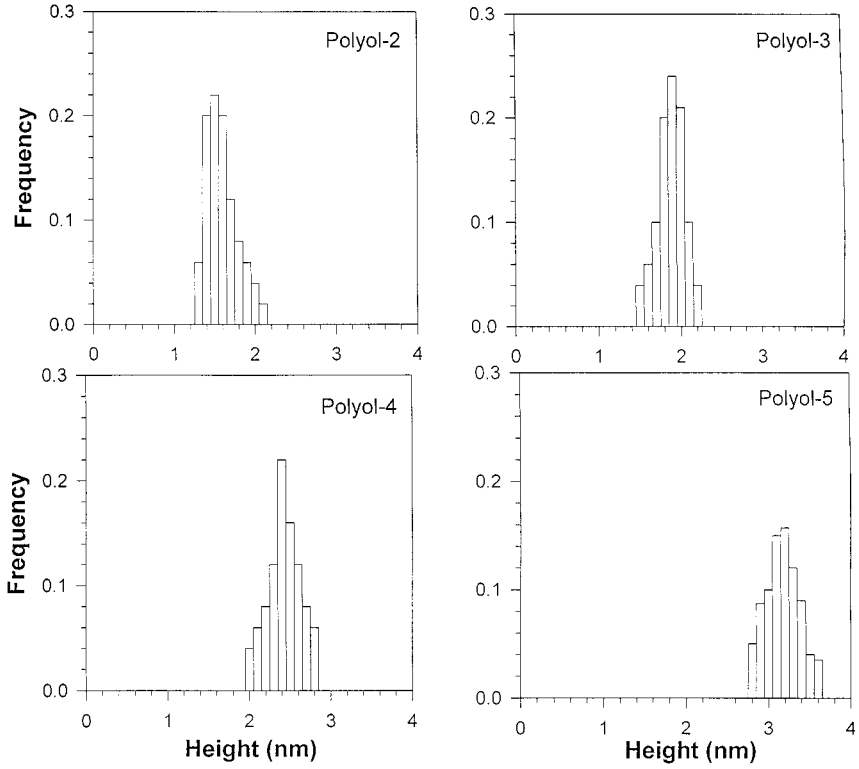

Figure 7 Height distribution of polyols from AFM.

compared to unity for a perfect hyperbranched molecule, confirms the presence of linear bis-MPA segments. Numerical simulations indicate that even in ideal structures highly folded branches are present at all stages of growth.[21] Being more flexible, the linear segments are especially likely to fold back on themselves and thus are positioned to readily crystallize. The observation that generation number affects neither the crystalline spacing nor the melting temperature supports this hypothesis. The X-ray and DSC results also reveal that the amount of crystallinity is low and the crystallites are small and/or imperfect.

Typical AFM phase images of polyols showed particles dispersed on the mica substrate (Fig. 6). Height scans revealed the particles to be on the order of 2 nm high, or approximately the dimension of a single polyol molecule. Distributions based on height measurements of 50 particles indicated a range of particle heights as anticipated for the broad molecular weight distribution (Fig. 7). The range overlapped from one polyol to another; however, the maximum in the distribution increased with the generation number from 1.5 nm for polyol-2 to 3.2 nm for polyol-5. Excellent agreement between the particle dimension from AFM height scans and the molecular diameter calculated from the theoretical molecular weight and density by assuming a spherical shape (Table IV) suggested that the polyols deposited as monolayers of spherical molecules. This is perhaps surprising because most models indicate that molecules of a low generation number are not spherical, although the shape rapidly approaches spherical between the first and third generations.[22,23] It may be that packing in the condensed state tends to promote a uniform, that is, spherical, shape of the molecules.

To obtain the lateral dimension of the particles in the AFM images, it was necessary to correct for the tip radius. Using the standard method for spherical particles[24] and a tip radius of 10 nm, a

Table IV Size of Hyperbranched Polyols

Designation	Calculated Diameter for Spherical Shape (nm)	Monolayer Thickness from AFM (nm)
Polyol-2	1.6	1.5 ± 0.4
Polyol-3	2.0	1.9 ± 0.4
Polyol-4	2.6	2.4 ± 0.4
Polyol-5	3.3	3.2 ± 0.4

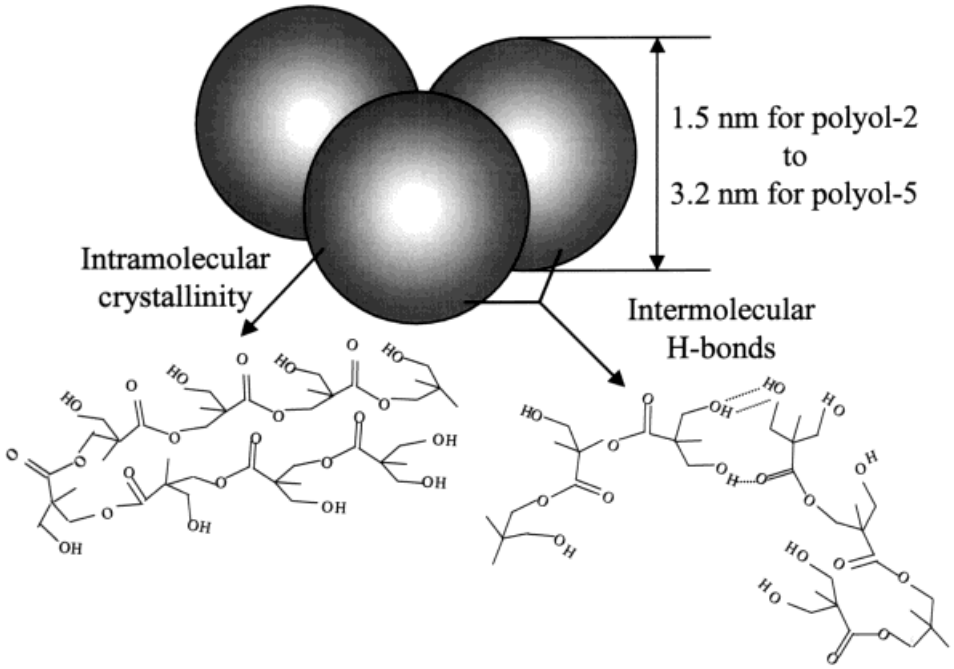

Figure 8 Schematic representation of the polyol structure.

minimum particle diameter of 15 nm was calculated, which is an order of magnitude larger than the diameter of a single molecule. The particles in the AFM images appear to be monolayer aggregates of spherical molecules. The polyols probably form aggregates in solution. Like solution aggregates of dendritic polymers,[1,25] aggregates of polyols are probably stabilized by hydrogen bonding of terminal groups.

Based on the various measurements, a hierarchical model of the solid-state polyol can be suggested (Fig. 8). The polyol molecules form monolayer aggregates when deposited from a dilute solution. The spherical shape of individual mole-

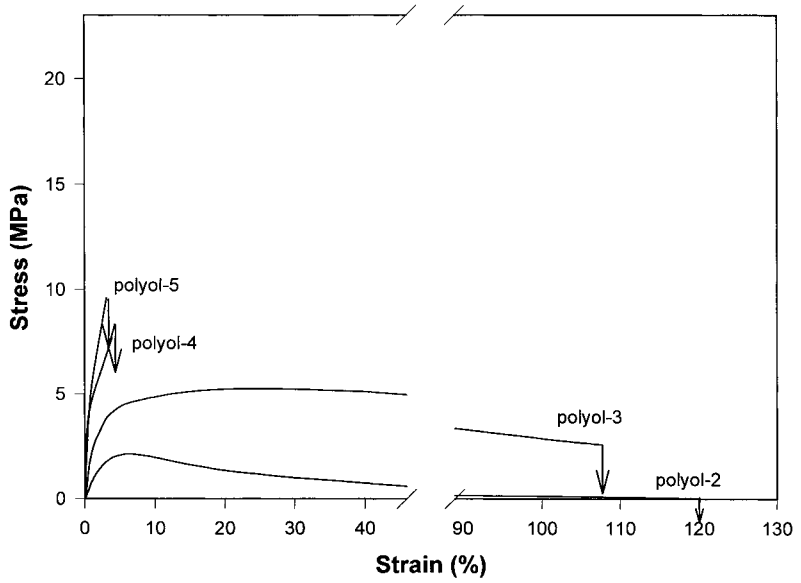

Figure 9 Effect of generation number on the stress–strain behavior of polyols.

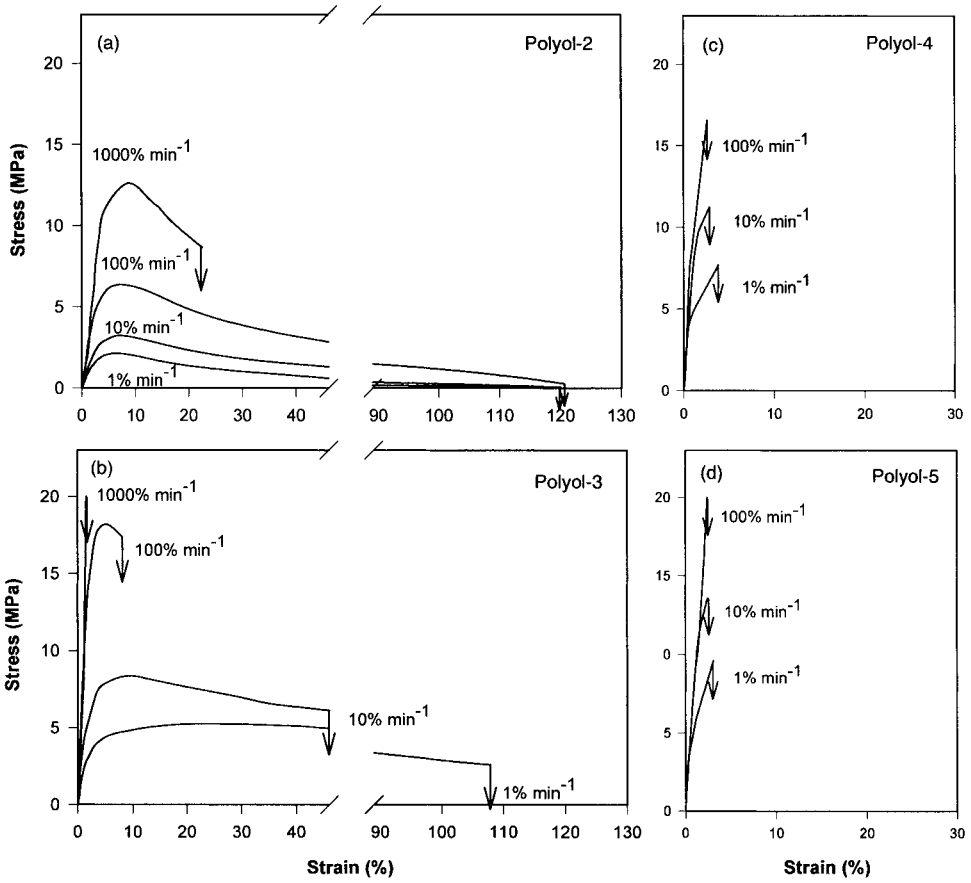

Figure 10 Effect of strain rate on the stress–strain behavior: (a) polyol-2; (b) polyol-3; (c) polyol-4; (d) polyol-5.

cules is indicated by the correspondence between the dimension obtained from AFM height images and the diameter calculated from the molecular weight for a spherical molecule. The small amount of crystallinity is attributed to linear segments that fold back on themselves and crystallize. Otherwise, the arms are disordered or amorphous as indicated by the prominent glass transition and low degree of crystallinity. Associations between molecules in the aggregate probably arise from intermolecular hydrogen bonding between terminal repeat units.

Stress–Strain Behavior

Polyols that were below the T_g were brittle and fractured at a strain of less than 5% (polyol-4 and polyol-5 in Fig. 9). Polyols that were above the T_g exhibited a maximum in the stress–strain curve with localized thinning of the specimen (polyol-2 and polyol-3 in Fig. 9). However, the neck did not stabilize. Instead, the neck became progressively thinner until it fractured. This behavior contrasts with typical thermoplastics where strain hardening stabilizes the neck and permits it to propagate along the gauge length. The behavior of the polyols is analogous to that of some ductile metals. Like the ductile metals, the polyols do not strain harden. This is consistent with their globular structure that does not permit the processes of chain extension and orientation that are the usual mechanisms of strain hardening. However, intermolecular associations, such as hydrogen bonding and possibly intermolecular crystallization of linear segments, provided connections between hyperbranched molecules. The yield stress reflected the force required to overcome these associations.

The effect of strain rate is illustrated for each of the polyols in Figure 10. The maximum stress always increased with strain rate and generation number. For polyol-2, the strain rate did not affect the mode of deformation, characterized by gradual thinning of the neck until it fractured at

an engineering strain above 100%, except for the highest strain rate. At a strain rate of 100%/min, the neck fractured after thinning only slightly and the fracture strain was correspondingly much lower. Polyol-3, which was closer to the T_g, exhibited a ductile-to-brittle transition. As strain rate increased, the neck thinned down less before fracturing, and the fracture strain decreased accordingly, until at the highest strain rate, brittle fracture preceded yielding. Increasing the strain rate effectively shifted the T_g to a higher temperature. In the case of polyol-3, the strain rate shifted the T_g from slightly below ambient temperature to above ambient temperature, and a ductile-to-brittle transition resulted. The effect of strain rate on the stress–strain behavior of the polyols that were below the T_g (polyol-4 and polyol-5) was to increase the fracture stress without significantly altering the fracture strain.

In summary, a study of hyperbranched polyols provided some insight into the structure–property relationships in these globular polymers. The primary thermal transition is the glass transition of the amorphous branched arms. Generation number has a major impact on the glass transition temperature. This is particularly significant for polyols based on unmodified bis-MPA because the glass transition is close to ambient temperature. Thus, a small decrease in T_g alters the behavior from brittle to ductile. A further consequence is the strong dependence of deformation behavior on strain rate. The polyols have a small amount of crystallinity that is probably associated with linear arm segments. Interactions between molecules are provided by hydrogen bonding of terminal repeat units. The intermolecular associations are strong enough to produce a yield stress in the tensile stress–strain curve of polyols that are above the glass transition temperature.

This research was generously supported by the Amoco Chemical Co.

REFERENCES

1. Tomalia, D. A.; Baker, H.; Dewald, J.; Hall, M.; Kallos, G.; Martin, S.; Roeck, J.; Ryder, J.; Smith, P. Polym J 1985, 17, 117.
2. Denkewalter, R. G.; Kolc, J. F.; Lukasavage, W. J. U.S. Patents 4289872, 1981; 4360646, 1982; 4410688, 1983.
3. Newkome, G. R.; Yao, Z.; Baker, G. R.; Gupta, V. K. J Org Chem 1985, 50, 2003.
4. Fréchet, J. M. J.; Hawker, C. J.; Gitsov, I.; Leon, J. W. Pure Appl Chem 1996, A33, 1399.
5. Tomalia, D. A.; Naylor, A. M.; Goddard, W. A. Angew Chem Int Ed Engl 1990, 29, 138.
6. Malmström, E.; Johansson, M.; Hult, A. Polym News 1997, 22, 128.
7. Voit, B. I. Acta Polym 1995, 46, 87.
8. Ihre, H.; Johansson, M.; Malmström, E.; Hult, A. In Advances in Dendritic Macromolecules; Newkome, G. R., Ed.; JAI: Greenwich, CT, 1996; Vol. 3, p 1.
9. Kim, Y. H.; Webster, O. W. J Am Chem Soc 1990, 112, 4592.
10. Malmström, E.; Johansson, M.; Hult, A. Macromolecules 1995, 28, 1698.
11. Mourey, T. H.; Turner, S. R.; Rubinstein, M.; Fréchet, J. M. J.; Hawker, C. J.; Wooley, K. L. Macromolecules 1992, 25, 2401.
12. Kim, Y. H.; Webster, O. W. Macromolecules 1992, 25, 5561.
13. Johansson, M.; Hult, A. J Coat Tech 1995, 67, 35.
14. Wooley, K. L.; Hawker, C. J.; Pochan, J. M.; Fréchet, J. M. J. Macromolecules 1993, 26, 1514.
15. Hult, A.; Malmström, E.; Johansson, M. In Polymeric Materials Encyclopedia; Salamone, J. C., Ed.; CRC: Boca Raton, FL, 1996; Vol. 5, p 3171.
16. Stutz, H. J Polym Sci Part B Polym Phys 1995, 33, 333.
17. Lal, J.; Trick, G. S. J Polym Sci Part A 1964, 2, 4559.
18. Oosterhof, H. A. Polymer 1974, 15, 49.
19. Stutz, H.; Illers, K.-H.; Mertes, J. J Polym Sci Part B: Polym Phys 1990, 28, 1483.
20. Liau, W.-B.; Boyd, R. H. Macromolecules 1990, 23, 1531.
21. Lescanec, R. L.; Muthukumar, M. Macromolecules 1990, 23, 2280.
22. Moreno-Bondi, M. C.; Orellana, G.; Turro, N. J.; Tomalia, D. A. Macromolecules 1990, 23, 910.
23. Gopidas, K. R.; Leheny, A. R.; Caminati, G.; Turro, N. J.; Tomalia, D. A. J Am Chem Soc 1991, 113, 7335.
24. Sheiko, S. S.; Eckert, G.; Ignat'eva, G.; Muzafarov, A. M.; Spickermann, J.; Räder, H. J.; Möller, M. Macromol Rapid Commun 1996, 17, 283.
25. Campagna, S.; Giannetto, A.; Serroni, S.; Denti, G.; Trusso, S.; Mallamace, F.; Micali, N. J Am Chem Soc 1995, 117, 1754.